The evolution of melt thermograms of HDPE, LLDPE and blended geomembranes incubated at 105°C

Ramy Awad, Mohamed S. Morsy & R. Kerry Rowe
Geoengineering Centre, Queen's- RMC, Canada

ABSTRACT: HDPE and LLDPE geomembranes are typically used as liners in various engineering applications including municipal solid waste landfills, brine ponds, and mining facilities. The liner temperature differs from one application to another and for some applications such as landfills containing aluminum production waste the temperature can exceed 85°C and in some cases, it can reach up to 143°C. It has been reported that the leachate temperature above the liner can exceed 80°C and in some cases in can exceed 100°C. This study focuses on the investigation of morphological changes associated with the subjection of five different 1.5 mm-thick geomembranes (two HDPE, two LLDPE and one blended polyolefin) incubated in air at 105°C in a forced-air oven for one month. The morphological changes are assessed via differential scanning calorimetry, the peak melting temperatures associated with lamellae thickening as well as crystallinity increased with testing time for all tested geomembranes. All geomembranes exhibited changes in melting endotherms from the unaged state upon annealing, exhibiting different features which are associated with crystalline regions forming during annealing and upon cooling from annealing temperature. The tie-molecule density was reduced upon annealing due to both lamellae thickening and the formation of crystalline regions just above the annealing temperature which accelerates the stress-crack growth. The reduction in tie-molecules density is counteracted by the tautness of remaining tie-molecules upon lamellae thickening. With further annealing, it is expected that the taut tie-molecules will slip and get incorporated in one lamellae hence accelerating stress-crack growth.

Keywords: geomembranes, HDPE, LLDPE, blended polyolefin, morphological change

1 INTRODUCTION

The decomposition of organic matter from municipal solid waste (MSW) is usually the primary source of heat generated in a landfill. This heat can affect the performance of the bottom liner, the cover, and the leachate collection system (Jafari et al. 2017). Aerobic conditions are the one cause of high temperature in a landfill (Rowe 1998). Air is introduced in a landfill during burial and the oxygen in the entrapped air reacts with methane releasing water, carbon dioxide and heat (Hao et al. 2017). Air can also be introduced in the landfill through excessive gas collection withdrawal which causes air to infiltrate into the landfill through cracks in the soil cover due to differential settlement or desiccation (Jafari et al. 2017). Aerobic biodegradation produces water, carbon dioxide and heat (Meraz and Dominguez 1998). Oxygen can also elevate the temperature in the landfill to 85°C and higher because of its contribution to combustion and smoldering at low oxygen levels (Jafari et al. 2017). The exothermal reactions from Aluminum production waste (APW) (Calder & Stark 2010) and bottom ash (Klein et al. 2001) can also excessively elevate the temperature in a landfill.

APW, raw municipal solid waste and industrial solid waste that contain aluminum can raise the temperature of MSW landfill to approx. 150°C (Calder & Stark 2010). Highly exothermic reactions occur when the aluminum waste comes in contact with alkaline water (pH ≥ 9) (e.g., from alkaline incinerator ash) (Petrovic and Thomas 2008). These exothermic reactions can hinder the anaerobic microbial activity and can pyrolysize the waste (Calder and Stark 2010). The reaction of aluminum with alkaline water produces flammable hydrogen gas and an immense amount of heat and in the presence of aluminum waste, it is probably the reaction that takes place in MSW landfill in the presence of aluminum waste. Stark et al.

(2011) and Jafari et al. (2017) observed temperatures of MSW landfills with aluminum waste in range of 88 to110°C.

The exposure of GMBs to air at high temperatures (95, 105 and 115°C) caused a change in polymer morphology that evolved with increasing the incubation duration and temperature and changed the stress-crack resistance (SCR) of the GMBs incubated at 105 and 115°C before the onset of oxidative degradation (Abdelaal et al. 2014).

The objective of this research is to examine: (1) the morphological changes associated with the incubation of five different GMBs: two 1.5-mm high-density polyethylene (HDPE) GMBs, two 1.5-mm linear low-density polyethylene (LLDPE), and one 1.5-mm blended GMB, and (2) the probable effect on mechanical properties with special emphasis on the density of tie-molecules which control stress crack growth rate. The polymeric GMBs were incubated in air inside a forced-air oven at 105°C.

High density polyethylene (HDPE) GMBs are typically composed of 96-98 % medium density polyethylene resin, 2-3 % carbon black (CB) and 0.25-1 % antioxidants and stabilizers (Hsuan et al. 2008). Linear low-density polyethylene (LLDPE) GMBs are typically manufactured from LLDPE resin of percentage reduced to 94-96% and additives increased to 0.25-3% (Koerner et al. 2005). Blended polyolefin GMB (BPO) is a proprietary polymer resin (Morsy and Rowe 2017). The molecular structure of HDPE and LLDPE are different. HDPE are characterized by having a low degree of short-chain branching (SCB) and LLDPE have more short-chain branching (SCB). SCB number and length directly affect the stress crack resistance (SCR), the melting points and the spherulite size (Bubeck and Baker 1982).

SCB number and length affects the stress crack resistance by controlling the density of the tie-molecules (molecules that connect different crystals and are critical for stress-crack resistance). Figure 1 shows an electron micrograph of a PE crystallized from the melt where interlamellar and interspherulitic tie-molecules are bridging between lamellae in the same spherulites and lamellae from adjacent spherulites, respectively. LLDPE usually has higher SCR than HDPE due to the presence of higher tie-molecules density. Microstructure of the polymer - controlled by branching- directly affects craze formation and stress-crack growth (SCG) (Bubeck and Baker 1982).

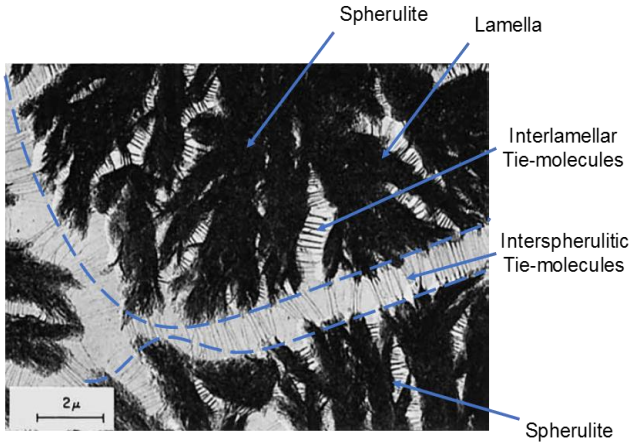

Figure 1. Electron micrograph of PE crystallized from the melt showing tie-molecules bridging between lamellae in a spherulite and lamellae from adjoining spherulites (modified after Keith et al. 1966)

The increase in short-chain branching lowers the density of the polymer since they are removed from the crystalline regions causing disruption in the chain folding (VanderHart and Perez 1986). Consequently, the density of the crystalline regions decreases, and the density of tie-molecules increase (Lustiger and Ishikawa 1991) hence the stress-crack resistance (Huang & Brown 1990, O'Connell et al. 2003).

Subjecting the GMB sample to a high temperature for a relatively long period (annealing) will cause the thickening of lamellae and the higher the incubation temperature the higher the thickening rate (Peterlin 1963). It has been established that annealing occurs via two procedures: one is the melting of the regions having their melting temperature below the annealing temperature and their reincorporation in larger crystals which have melting temperatures higher than the annealing temperatures (unmolten) hence causing thickening of the crystals. The other process is the migration of the amorphous regions (solid-state crystalline growth) (Petermann et al. 1976).

2 EXPERIMENTAL INVESTIGATION AND EXAMINED GEOMEMBRANES

The GMB coupons (9 cm × 18 cm) were placed in a glass jar and then incubated in air inside a forced-air oven at 105°C. The jar was not covered during the incubation to avoid any air pressure build-up. To collect the samples, the jar was removed from the oven and left to cool down in room temperature for 3 hours before collecting the samples (1 cm × 1 cm). The samples are then tested 24 hours after collection.

Melting and crystallization temperatures of the GMB samples were measured via ASTM (E794) and the melting endotherms were obtained via ASTM (E793) using a differential scanning calorimeter (DSC). The testing program is set to equilibrate the sample at 0°C and then gradually raise the temperature to 200°C at a rate of 10°C/ min.

Two 1.5 mm HDPE GMBs (MyE15 and MyF3), both from manufacturer "y" were tested. Two 1.5 mm LLDPE GMBs (LxD15 and LxE15), both provided from manufacturer "x", were also tested. Finally, a blended polyolefin (BPO) 1.5 mm-thick white on one side GMB (BzSW15), provided by manufacturer "z" was tested. Figure 2 is a schematic showing a generic melting enthalpy which is the area of the shaded area, the figure also shows the peak melting temperature. The initial peak melting temperatures as well as initial crystallinity for the five tested GMBs are presented in Table 1. The initial melting thermograms are shown in Figure 3 for MyE15, MyF3, LxD15, LXE15 and BzSW15. The percent crystallinity (X_c %) is calculated by dividing the melting enthalpy of the polymer by 290 J/g which is the melting enthalpy of perfectly crystalline PE viz:

$$X_c\ (\%) = [(\Delta H) / (\Delta H_{100})] \times 100$$

where, ΔH is the melting enthalpy representing the integrated area between the melted endotherm and arbitrary baseline taken from 60 to 160°C. ΔH_{100} is the melting enthalpy of a perfect crystalline polyethylene (290 J/g).

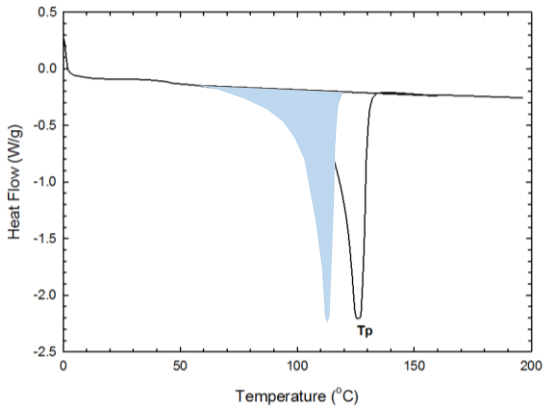

Figure 2. Schematic showing a melting endotherm thermogram, shaded area is melting enthalpy and Tp is the peak melting thermogram.

Table 1. Peak melting temperature (T_m °C) and crystallinity percentage (%) for the five tested GMBs

GMB	MyE15	MyF3	LxD15	LxE15	BzSW15
T_m (°C)	127.33	125.62	123.58	123.63	126.06
X_c (%)	52.12	54.78	45.70	40.61	31.51

The crystallinity for the HDPE GMBs was the highest, and was lowest for BPO GMBs. The peak melting temperatures for the two HDPE and the blended GMBs are within the same range and higher than that of the two LLDPEs. The relatively lower crystallinity for LLDPE GMBs is due to the relatively higher degree of short-chain branching (SCB). The relatively shorter long-periods of LLDPE GMBs is also caused by the relatively higher degree of SCB.

Evolution of lamellae thickness with aging time is indicative of morphological changes and can be calculated using Gibbs and Thomson Equation (Włochowicz and Eder 1984) viz:

$$L_c\ (nm) = (0.627 \times 414.2)/(414.2 - T)$$

where, L_c is the lamella thickness (nm) and T is the absolute peak melting temperature (K) and 414.2 K is the melting temperature of an infinitely thick perfect PE crystal.

3 RESULTS

The development of melt thermograms with ageing time at 105°C for HDPE (MyE15, MyF3), LLDPE (LxD15, LXE15) and BPO (BzSW15) are shown in Figures 4, 5, and 6, respectively. The evolution of crystallinity and lamellae thickness with ageing time for all GMBs are presented in Figures 7 and 8, respectively.

The evolution of melt thermograms with ageing for MyE15 (Figure 4a) involved a substantial increase in melt enthalpy, and hence crystallinity, with ageing time and is very evident from as early as 6 days. Crystallinity increased from 52 to 60% in 12 days and then slowly increased to 60.8% at 33 days without reaching a maximum value (Figure 7). There was no substantial increase in lamellae thickness with aging time based on peak melting temperature (T_p) measurement despite the relatively large scatter (Figure 8). The evolution of γ and β regions (Figure 4a) - where γ occurs below the annealing temperature (T_A = 105°C) and β occurs slightly above T_A- are related to crystals that are formed below T_A and crystals that are thickened above T_A, respectively (Lu et al. 1992a). The thickened crystals above T_A (β) were not considered in the evolution of lamellae thickening measurement since there was no change in the peak melting temperature for the testing period despite the high data scatter.

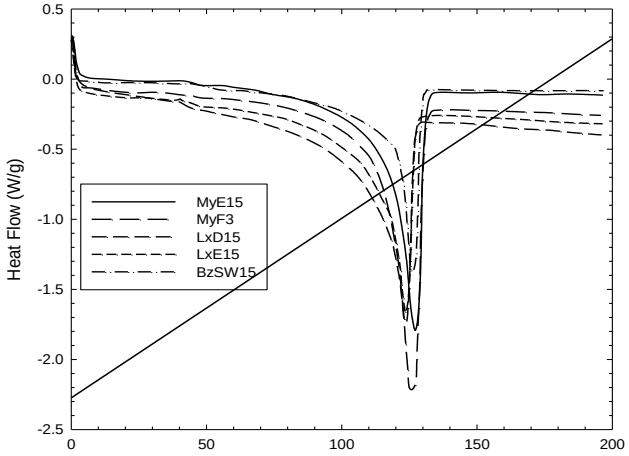

Figure 3. Melt thermograms of the unaged GMBs. Inclined solid line represents the increase in melting temperature from 0 to 200°C at a rate of 10°C/min.

The melt thermogram for MyF3 shows the evolution of the two regions γ and β same as MyE15 (Figure 4b). There was an increase in crystallinity from 54.8 to 58% in the first 12 days of incubation and then remained constant for the rest of the testing period (Figure 7). Lamellae thickness increased in the first six days of incubation and remained constant for the remaining testing period (Figure 8).

The melting thermogram for both LxD15 and LxE15 (Figures 5 a and b, respectively) are different from those of HDPE GMBs showing more thickening of crystals above T_A. Crystallinity of LxD15 started increasing after 12 days incubation (Figure 7) from 45.9 to 47.2%. Crystallinity of LxE15 started increasing right from the beginning of incubation 40.6 to 42.5% after 12 days of incubation and then increased slowly from 42.5 to 43.5% after 33 days. The evolution of lamellae thickening of LxD15 and LxE15 were almost identical, the lamellae thickness for both GMBs increased relatively fast in the first 9 days of incubation, the thickening then slowed down for the rest of the incubation period without reaching a maximum value.

Blended GMB (BzSW15) showed a slow increase in crystallinity with time for the first 19 days (Figure 7) and the increase in crystallinity accelerated for the rest of the testing period. Lamellae thickness also increased, relatively fast in the first three days of incubation and relatively slower afterwards without reaching a maximum value for the rest of the testing period.

4 DISCUSSION

The kinks below and above the annealing temperature (T_A = 105°C), γ and β regions respectively are associated with the crystalline regions melted during annealing and recrystallized upon cooling, and the crystals that form and/or thicken above the annealing temperature, respectively (Lu et al. 1992b).

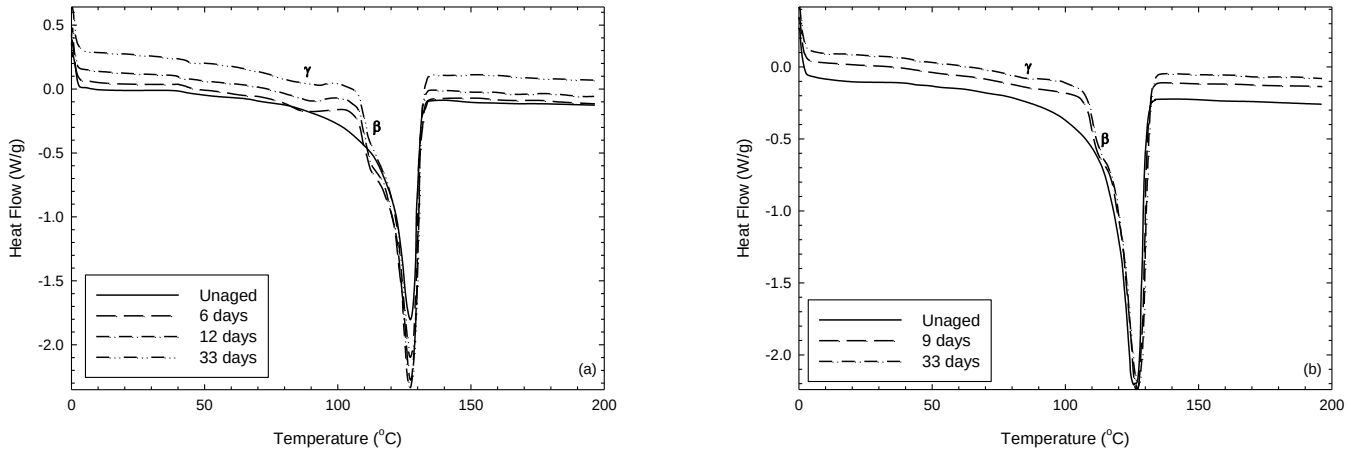

Figure 4. (a) Melt thermograms of (a) MyE15 and (b) MyF3 for unaged samples and after various days of incubation. Thermograms are vertically offset to clearly show the difference in the curves shapes.

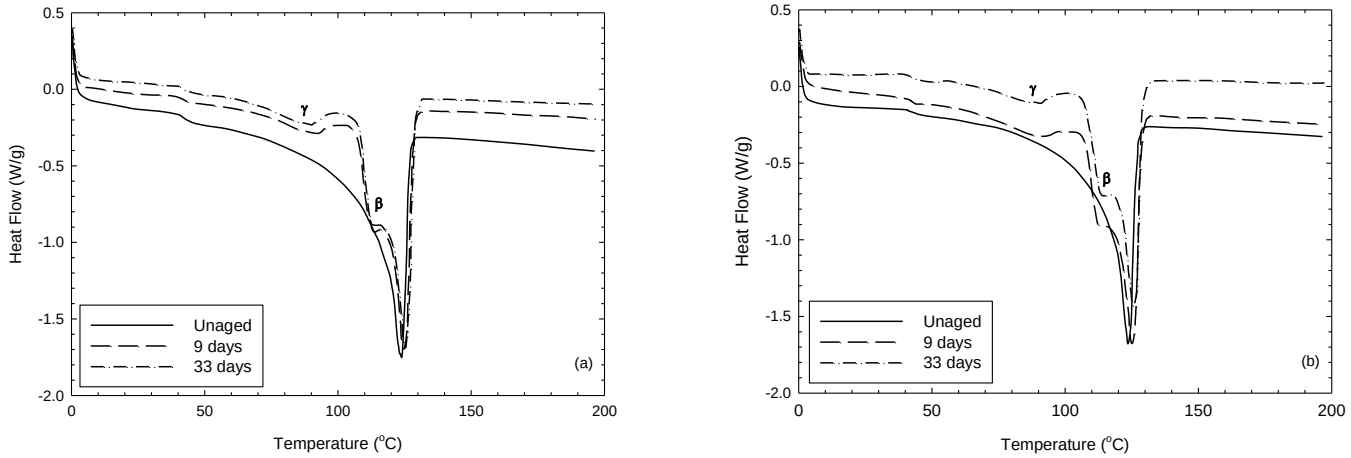

Figure 5. (a) Melt thermograms of (a) LxD15 and (b) LxE15 for unaged samples and after various days of incubation. Thermograms are vertically offset to clearly show the difference in the curves shapes.

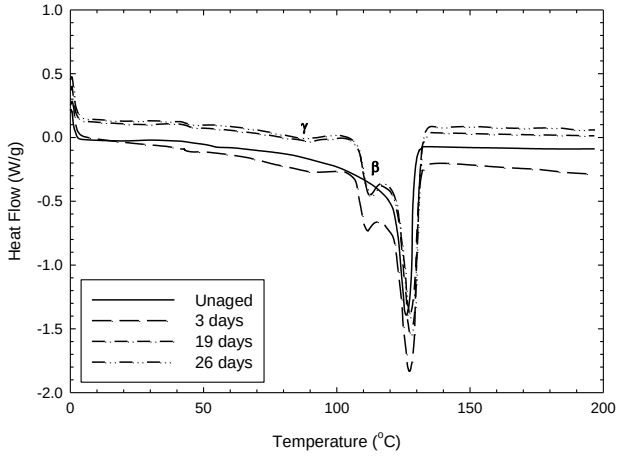

Figure 6. Melt thermograms of BzSw15 for unaged samples and after various days of incubation. Thermograms are vertically offset to clearly show the difference in the curves shapes.

For the case of HDPE GMBs (MyE15 and MyF3) the β region is relatively small indicating that crystals formed and thickened above T_A are relatively small. For the LLDPE GMBs (LxD15 and LxE15), the β region is larger than that for HDPE GMBs, since the crystals formed during annealing are formed between the short-chain branches (Lu et al. 1992b). The blended GMB (BzSW15) showed two peaks in the DSC melting thermogram indicating that a large portion of the crystals that formed during annealing above T_A were formed between the short chain branches - which seems from the relatively low initial crystallinity of the GMB material - that the volume between the short chain branches is bigger than for HDPE and LLDPE GMBs. The peak melting temperature at β region coincides for BzSW15 with the peak melting temperature (112°C) associated with branched polyethylene while the higher peak melting temperature (126.2°C) is associated with linear polyethylene.

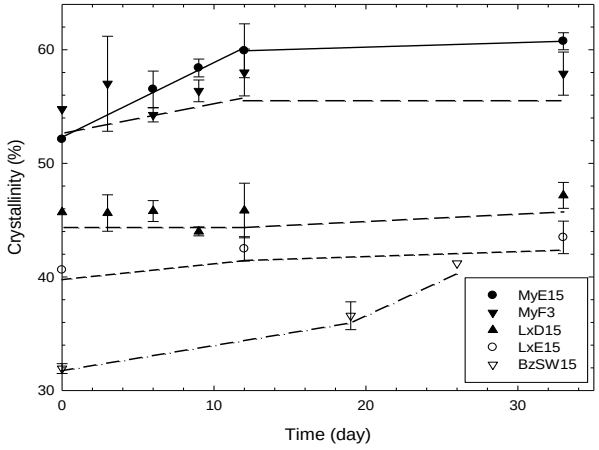

Figure 7. Evolution of crystallinity with aging time for the five tested GMBs at 105°C incubated in air. Error bars represent data range.

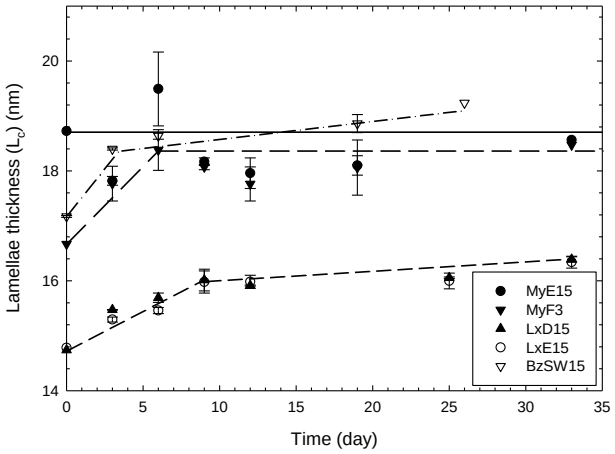

Figure 8. Evolution of lamellae thickness with aging time for the five tested GMBs at 105°C incubated in air. Error bars represent data range

Two competing processes occur during annealing and affect the density of tie-molecules which are responsible for stress crack growth: (a) upon annealing, tie-molecules are absorbed by one of the attaching thickening crystals and the molten molecules that recrystallize during annealing (β region) tend to have fewer tie-molecules when compared to the quenched state (Lu et al. 1992b) eventually increasing the rate of disentanglement and (b) upon annealing, the crystals size increase and the tie-molecules become taut which increases the entanglement, also the portion material which has a melting temperature lower than T_A and that doesn't crystallize during annealing but rather crystallize upon cooling from T_A (γ region) tend to form tie-molecules which increases the entanglement noting that the tie-molecules' density formed in γ region is still lower than their density in the unaged (as quenched from the melt) state.

For the two HDPE GMBs, the amplitude of both γ and β regions increased upon annealing (Figures 4a and b) which indicates that the density of tie-molecules in β region has decreased and increased in γ region to an extent lower than that for the unaged state as previously indicated. Also, the increase in crystal-

linity for both GMBs (Figure 7) and the increase in lamellae thickness upon ageing for MyF3 (Figure 8) measured for the linear portion of the polymer from the melt thermogram suggest that the overall density of tie-molecules for both GMBs will decrease during annealing with MyF3 being more subjected to higher reduction in tie-molecules density than MyE15 when compared to unaged tie-molecules density for both GMBs. For the two LLDPE GMBs, the amplitudes of both γ and β regions are relatively high compared to HDPE GMBs indicating that a relatively large portion of crystalline lamellae having melting temperature lower than T_A have recrystallized during annealing in volumes between short chain branches yielding lower density of tie-molecules compared to the as-quenched state (β region). The increase in lamellae thickness (Figure 8) for LxE15 and LxD15 and the relatively high amplitude of β regions suggest that the overall density of tie-molecules decreased upon annealing. For the BPO GMB, the increase in the amplitude of β region upon annealing is higher than the increase in the amplitude of γ region to the extent of creating another melting peak coinciding with branched polyethylene. It is expected that the loss in tie-molecules density in comparison with the unaged density will be higher than the tie-molecules reduction for LLDPE and HDPE compared to their respective unaged densities.

The disentangling effect caused by reduction in tie-molecules density for tested GMBs except for MyE15 due to thickening can be counteracted with tautness of remaining tie molecules that are better pinned to the adjacent crystals, which will slow the disentanglement. Upon further annealing and thickening of lamellae, it is expected that the tie-molecules will slip from one of the attaching lamella and become incorporated in the other lamella hence accelerating the disentanglement and consequently the stress-crack growth.

When subjected to elevated temperatures, HDPE, LLDPE and BPO GMBs experienced morphological changes which probably caused a reduction in tie-molecules' density hence a possible reduction in the stress-crack resistance of the GMBs.

5 CONCLUSIONS

Five geomembranes (two HDPE, two LLDPE and one BPO) were incubated in air inside a forced-air oven at 105°C to evaluate the morphological changes associated with annealing at high temperatures. The following conclusion were drawn from the melt thermograms:

1- The amplitudes of γ and β regions for HDPE geomembranes were relatively low given the very small short chain branches density and consequently the small probability of crystalline regions being formed around them. The increase in crystallinity for MyE15 and MyF3, and the increase in lamellae thickness for MyF3 for few days after incubation is indicative of a reduction in tie-molecules density, tie-molecules being responsible for controlling stress-crack growth, the higher the density of tie-molecules, the slower is the disentanglement and the stress-crack growth.
2- The amplitudes of γ and β regions for LLDPE geomembranes were more pronounced than for HDPE geomembranes due to crystallization in the volume between the short chain branches; although it is expected that tie-molecules were formed in the γ regions, it is also expected that their density in γ region are lower than that the as-quenched (initial) state. Also, the relatively high amplitude of β region for the LLDPE geomembranes is indicative of crystalline regions formed at temperatures higher than the annealing temperature. These crystalline regions are expected to have very low densities of tie-molecules. Furthermore, due to lamellae thickening for both LLDPE geomembranes, it is expected that the tie-molecule density – especially those associated with the linear portion of the copolymer – will be reduced.
3- β region for the blended geomembrane was more pronounced that γ region and creating a second melting peak which coincided with branched polyethylene portion of the resin. It is expected that density of tie-molecules was reduced due to the formation of β region and due to lamellae thickening of the linear portion of the resin.
4- The thickening of lamellae and the increase in tautness of tie-molecules can be expected to counteract the reduction in stress-crack resistance caused by the reduction in tie-molecules density upon annealing. With further annealing, it is expected that the taut tie-molecules will slip and get incorporated in one of the attaching lamellae which will accelerate the stress-crack growth.

ACKNOWLEDGEMENTS

The research reported in this paper was supported by a Natural Sciences and Engineering Research Council of Canada (NSERC) grant (A1007) to Dr. R.K. Rowe. The equipment used was funded by Canada Foundation for Innovation (CFI) and the Government of Ontario's Ministry of Research and Innovation

REFERENCES

Abdelaal, F. B., Rowe, R. K., Hsuan, Y. G., & Awad, R. (2015). Effect of high temperatures on the physical and mechanical properties of HDPE geomembranes in air. *Geosynthetics International*, *22*(3), 207-224.

ASTM. (2006). E793,"*Standard test method for enthalpies of fusion and crystallization by Differential Scanning Calorimetry*.

ASTM, E. 794 (2001). *Standard Test Method for Melting and Crystallization Temperatures by Thermal Analysis*.

Bubeck, R. A., & Baker, H. M. (1982). The influence of branch length on the deformation and microstructure of polyethylene. *Polymer*, *23*(11), 1680-1684.

Calder, G. V., & Stark, T. D. (2010). Aluminum reactions and problems in municipal solid waste landfills. *Practice Periodical of Hazardous, Toxic, and Radioactive Waste Management*, *14*(4), 258-265.

Hao, Z., Sun, M., Ducoste, J., Benson, C. H., Luettich, S., Castaldi, M. J., & Barlaz, M. A. (2017). Heat Generation and Accumulation in Municipal Solid Waste Landfills. *Environmental Science & Technology*.

Hsuan, Y. G., Schroeder, H. F., Rowe, K., Müller, W., Greenwood, J., Cazzuffi, D., & Koerner, R. M. (2008, September). Long-term performance and lifetime prediction of geosynthetics. In *Proceeding of EuroGeo 4-4th European Geosynthetics Conference.*

Huang, Y. L., & Brown, N. (1990). The dependence of butyl branch density on slow crack growth in polyethylene: kinetics. *Journal of Polymer Science Part B: Polymer Physics*, *28*(11), 2007-2021.

Jafari, N. H., Stark, T. D., & Thalhamer, T. (2017). Progression of Elevated Temperatures in Municipal Solid Waste Landfills. *Journal of Geotechnical and Geoenvironmental Engineering*, 05017004.

Keith, H. D., Padden, F. J., & Vadimsky, R. G. (1966). Intercrystalline links in polyethylene crystallized from the melt. Journal of Polymer Science Part B: Polymer Physics, 4(2), 267-281.

Klein, R., Baumann, T., Kahapka, E., & Niessner, R. (2001). Temperature development in a modern municipal solid waste incineration (MSWI) bottom ash landfill with regard to sustainable waste management. *Journal of Hazardous Materials*, *83*(3), 265-280.

Koerner, R. M., Hsuan, Y. G., & Koerner, G. R. (2005). Geomembrane lifetime prediction: unexposed and exposed conditions. *GRI White Paper*, *6*.

Lu, X., McGhie, A., & Brown, N. (1992a). The dependence of slow crack growth in a polyethylene copolymer on test temperature and morphology. *Journal of Polymer Science Part B: Polymer Physics*, *30*(11), 1207-1214.

Lu, X., Qian, R., McGhie, A. R., & Brown, N. (1992b). The effect of annealing on slow crack growth in an ethylene-hexene copolymer. *Journal of Polymer Science Part B: Polymer Physics*, *30*(8), 899-906.

Lustiger, A., & Ishikawa, N. (1991). An analytical technique for measuring relative tie-molecule concentration in polyethylene. *Journal of Polymer Science Part B: Polymer Physics*, *29*(9), 1047-1055.

Meraz, L., & Dominguez, A. (1998). A calorimetric description of the digestion of organic matter in landfills. *The Chemical Educator*, 3(6), 1-6.

Morsy, M. S., & Rowe, R. K. Performance of Blended Polyolefin Geomembrane in Various Incubation Media Based on Std-OIT. In *Geotechnical Frontiers 2017* (pp. 1-10).

O'Connell, P. A., Bonner, M. J., Duckett, R. A., & Ward, I. M. (2003). Effect of molecular weight and branch content on the creep behavior of oriented polyethylene. *Journal of applied polymer science*, *89*(6), 1663-1670.

Peterlin, A. (1963). Thickening of polymer single crystals during annealing. *Journal of Polymer Science Part B: Polymer Letters*, *1*(6), 279-284.

Petermann, J., Miles, M., & Gleiter, H. (1976). Growth of polymer crystals during annealing. *Journal of Macromolecular Science, Part B: Physics*, *12*(3), 393-404.

Petrovic, J., & Thomas, G. (2008). Reaction of aluminum with water to produce hydrogen. *US Department of Energy*, 1-26.

Rowe, R. K. (1998, March). Geosynthetics and the minimization of contaminant migration through barrier systems beneath solid waste. In *Proceedings of the 6th International Conference on Geosynthetics, Atlanta, Ga* (pp. 25-29).

Stark, T. D., Martin, J. W., Gerbasi, G. T., Thalhamer, T., & Gortner, R. E. (2011). Aluminum waste reaction indicators in a municipal solid waste landfill. *Journal of Geotechnical and Geoenvironmental Engineering*, *138*(3), 252-261.

VanderHart, D. L., & Perez, E. (1986). A carbon-13 NMR method for determining the partitioning of end groups and side branches between the crystalline and noncrystalline regions in polyethylene. *Macromolecules*, *19*(7), 1902-1909.

Włochowicz, A., & Eder, M. (1984). Distribution of lamella thicknesses in isothermally crystallized polypropylene and polyethylene by differential scanning calorimetry. *Polymer*, *25*(9), 1268-1270.